Supporting Information:

Transient EPR reveals triplet state delocalization in a series of cyclic and linear π-conjugated porphyrin oligomers

Claudia E. Tait,[†] Patrik Neuhaus,[‡] Martin D. Peeks,[‡] Harry L. Anderson,[‡] and Christiane R. Timmel[†,*]

[†]Department of Chemistry, Centre for Advanced Electron Spin Resonance, University of Oxford, South Parks Road, Oxford OX1 3QR, UK.

[‡]Department of Chemistry, Chemistry Research Laboratory, University of Oxford, 12 Mansfield Road, Oxford OX1 3TA, UK.

Table of Contents:

Experimental Methods

Sample preparation

The zinc porphyrin oligomers (**P1** to **P6**) and the porphyrin ring (***c*-P6**) depicted in Figure 1 of the main text were synthesized as described below. The EPR measurements were performed on 50–200 μM solutions in MeTHF: pyridine 10:1. The measurements on the oligomers bound to the template were performed in toluene, since coordinating solvents interfere with the binding of the template. The solutions were degassed by several freeze-pump-thaw cycles and frozen in liquid N_2.

Time-resolved EPR

The time-resolved EPR experiments were performed at X-band on a Bruker Elexsys 680 spectrometer equipped with a helium gas-flow cryostat from Oxford instruments. Laser excitation at 532 nm was provided by the second harmonic of an Nd:YAG laser (Surelite Continuum) with a repetition rate of 10 Hz. Light depolarized with an achromatic depolarizer was used unless otherwise stated. TR-EPR experiments were performed by direct detection with the transient recorder without lock-in amplification; the microwave power was 0.2 mW. The laser background signal was removed by 2D baseline-correction determined based on the off-resonance transients. The spectra were integrated over the first 2 μs after the laser flash. Experiments were typically performed at 20 K, but no changes in the spectra were observed at temperatures between about 100 and 5 K.

Experiments with different excitation wavelengths were performed with an Opotek Opolette Optoparametric Oscillator (OPO) tunable laser (20 Hz repetition rate) at wavelengths corresponding to the region of the Q-bands in the UV-Vis spectra (see Figure S1). For the magnetophotoselection measurements the light was polarized with a Glan-Thompson polarizer.

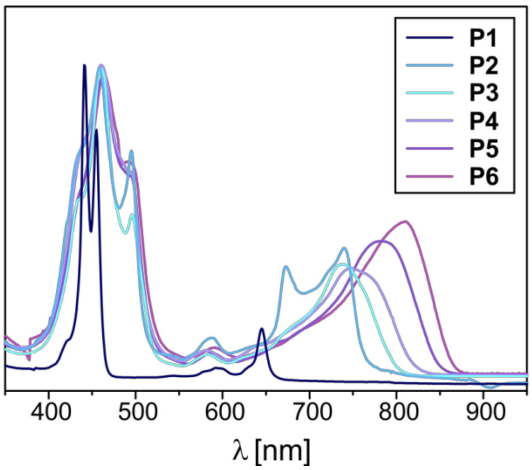

Figure S1. Room temperature UV-Vis spectra recorded in MeTHF:pyridine 10:1.

Pulse EPR

X-band pulse EPR measurements were performed on a Bruker Elexsys 680 spectrometer with a Bruker EN 4118X-MD4 resonator. The measurements were performed at 20 K and with laser excitation as previously described.

The repetition rate of the pulse experiments was determined by the laser repetition rate of 10 Hz (20 Hz for measurements with the OPO). Radical signals were removed with the use of a saturating microwave pulse preceding the laser flash.

^{1}H Mims ENDOR spectra were recorded with the pulse sequence $\frac{\pi}{2} - \tau - \frac{\pi}{2} - T - \frac{\pi}{2} - \tau - \text{echo}$ with mw pulse lengths of $t_{\pi/2}$=24 ns, τ =120, 160, 200 ns and a radiofrequency pulse length of 15 μs; the RF power was adjusted based on a nutation experiment. The ENDOR spectra were recorded at the canonical field positions of the triplet state EPR spectrum; spectra were recorded for three different τ values (120, 160 and 200 ns) and summed to prevent distortions by blind spots.

Spectral Analysis

The spin-polarized powder triplet state spectra were simulated using EasySpin's *pepper* routine.[1] The zero-

field splitting parameters *D* and *E* as well as the relative population probabilities at zero-field were determined by least-square fitting of the experimental transient EPR data. The energy ordering of the triplet sublevels was chosen as |Z|>|X|>|Y|.

The relative orientations of the zero-field splitting tensor orientations and the optical transition dipole moments was determined based on the polarization ratio calculated from the magnetophotoselection data. The polarization ratio is defined as:[2-3]

$$P_i = \frac{I_i^{\parallel} - I_i^{\perp}}{I_i^{\parallel} + I_i^{\perp}} \qquad (1)$$

where $I_i^{\parallel/\perp}$ are the intensities of the derivative EPR signal for excitation with light polarized parallel or perpendicular to the magnetic field at the field positions corresponding to the X, Y or Z orientation of the ZFS tensor. The polarization ratio was calculated by integration of the low and high field canonical regions of the derivative spectra; standard deviations were estimated by considering different regions for the integration (derivative signal maximum ±0.05-0.40 mT).

The values of the proton hyperfine couplings along the principal axes of the ZFS tensor were determined by Gaussian deconvolution of the ENDOR spectra.

Computational methods

DFT geometry optimizations of the triplet excited state structures for **P1** to **P6** and for **P2·T6** to **P4·T6** were performed in ORCA[4-5] with the BP86 functional and the SV(P) basis set using the RI approximation with the auxiliary SV/C basis set. The $Si(C_6H_{13})_3$ groups were replaced by hydrogen atoms and the resulting structures were optimized without symmetry constraints. Calculations of the zero-field splitting interaction were performed according to a procedure published by Sinnecker et al.,[6] using the B3LYP functional and the EPRII basis set[7] and calculating the spin-spin contribution to the ZFS using UNO determinants. Calculations of the zero-field splitting parameters could only be performed for systems with up to four porphyrin units, calculations on the larger systems were computationally not feasible. The results were compared to calculations with the BP86 and BHLYP functional to evaluate the extent of the self-interaction error and no significant difference was found. The spin density distributions for the linear oligomers are shown in Figure S2.

The hyperfine parameters were calculated with the B3LYP functional and the EPRII basis set, purposely developed for the calculation of EPR hyperfine interaction values, for the C, N and H nuclei[7-9] and the 6-31G(d) basis set for Zn.

The DFT calculations for **P3** predict an uneven spin density distribution with increased spin density on the central porphyrin unit. The predicted ratio of spin densities on the three porphyrin units depends on the amount of exact Hartree-Fock exchange included in the DFT functional. A calculation with the GGA (generalized gradient approximation) functional BP86 predicts a spin density distribution of 0.26:0.48:0.26 over the three porphyrin units, while the hybrid functional B3LYP, containing 20% of exact exchange and 80% of DFT exchange, predicts a distribution of 0.19:0.62:0.19. Variation of the contribution of exact exchange in the B3LYP functional in the range from 10% to 40% leads to variations of the relative spin density on the central porphyrin unit from 0.54 to 0.74. The best agreement of calculated and experimental hyperfine couplings is obtained for 20% exact exchange, corresponding to the standard B3LYP functional. This amount of exact exchange almost corresponds to the optimal mixing ratio of exact and DFT exchange believed to yield results close to chemical accuracy (25%).[10]

DFT also predicts uneven spin density distributions for **P4**, **P5** and **P6**, with the spin density mainly localized on the two central porphyrin units for even *N* and on the central porphyrin unit for odd *N*. The ratios of spin densities resulting from B3LYP/EPRII calculations (20% exact exchange) correspond to 0.10 : 0.40 : 0.40 : 0.10 for **P4**, 0.04 : 0.19 : 0.54 : 0.19 : 0.04 for **P5** and 0.02 : 0.10 : 0.38 : 0.38 : 0.10 : 0.02 for **P6**. The BP86 functional again predicts different spin density distributions, which are slightly more spread out over the porphyrin array due to the self-interaction error affecting DFT calculations with functionals only containing DFT exchange.[11]

The changes in ZFS parameters for different geometries of the linear oligomers were investigated by considering the SOMOs. The quasi-restricted molecular orbitals from single-point calculations performed at B3LYP/EPRII level for the porphyrin monomer, dimer, trimer and tetramer are shown in Figure S3. The corresponding orbitals of the templated oligomers are shown in Figure S4. The SOMOs localized using the Pipek-Mezey scheme[12] are also shown and were used to separate the Coulomb and exchange contribution to the *D*-value.

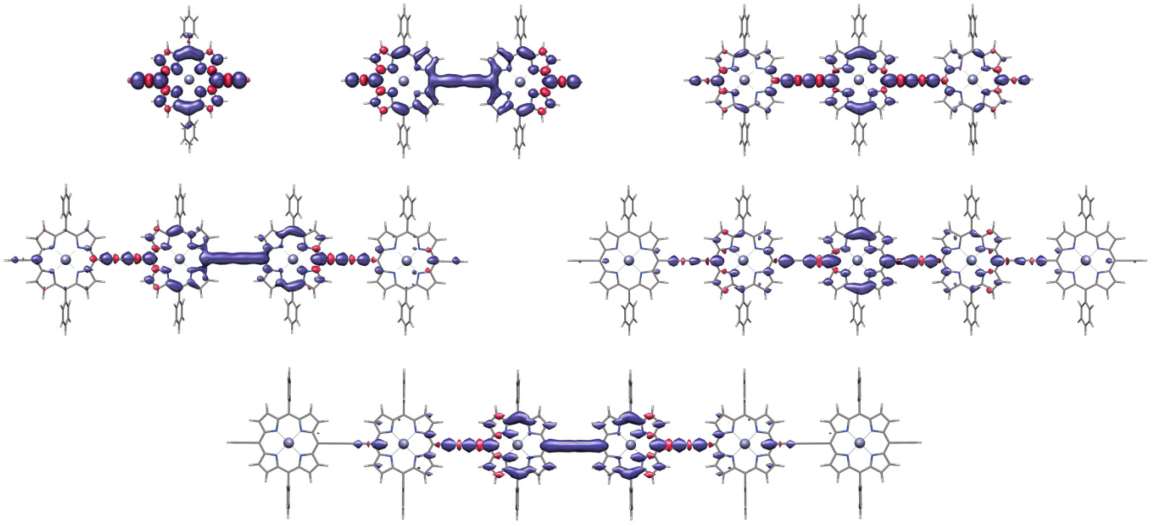

Figure S2. Spin density distributions in the first excited triplet state calculated at B3LYP/EPRII level for the optimized geometries of **P1** to **P6**.

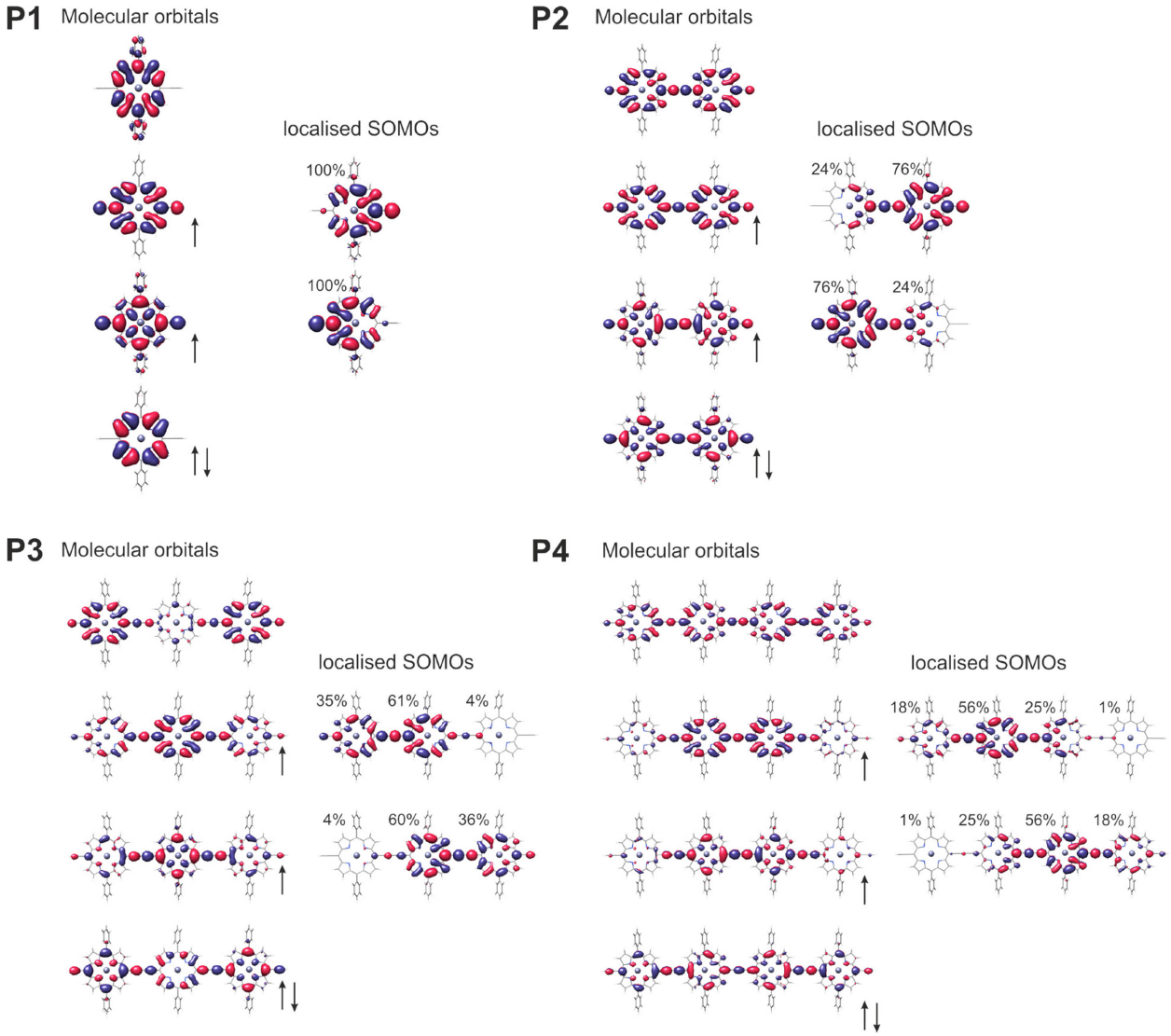

Figure S3. Plots of the frontier quasi-restricted molecular orbitals and of the localized SOMOs calculated with B3LYP/EPRII for **P1**, **P2**, **P3** and **P4**. The populations of the SOMOs on the different porphyrin units are indicated as percentages. The arrows indicate the electrons occupying each orbital. The small differences in population distributions in the two SOMOs for each molecule arise from deviations of the optimized geometry from symmetry, identical populations are obtained from calculations on symmetrized geometries.

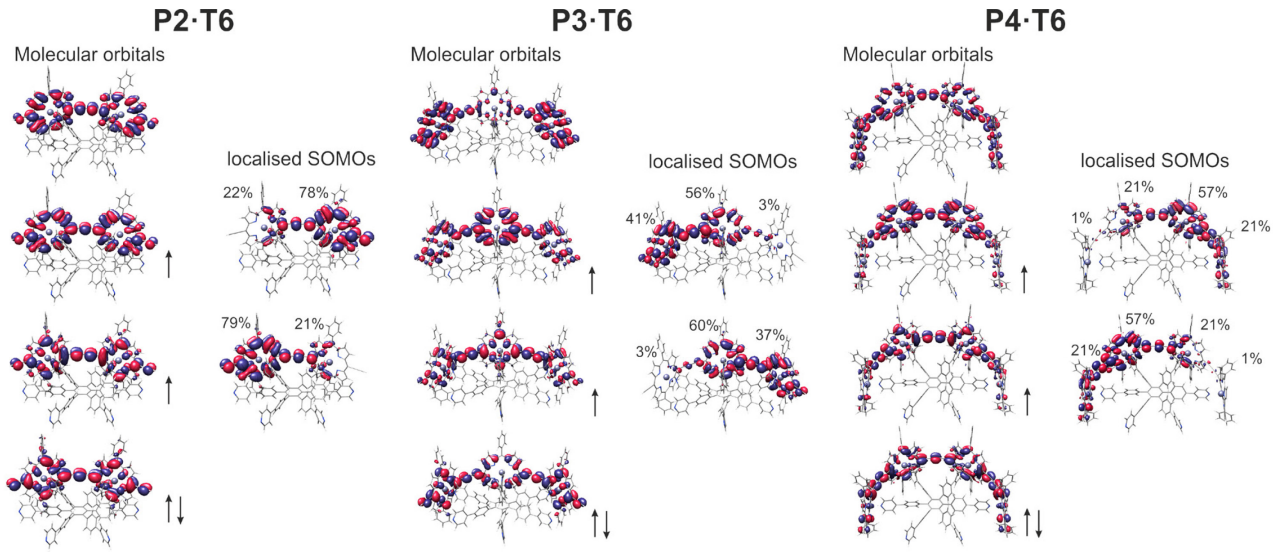

Figure S4. Plots of the frontier quasi-restricted molecular orbitals and of the localized SOMOs calculated with B3LYP/EPRII for **P2·T6**, **P3·T6** and **P4·T6**. The populations of the SOMOs on the different porphyrin units are indicated as percentages. The arrows indicate the electrons occupying each orbital.

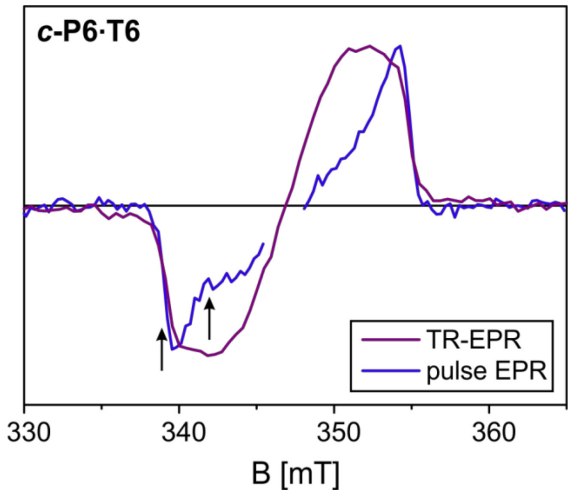

Figure S5. Comparison of the transient and echo-detected EPR spectra of ***c*-P6·T6**. The central part of the field sweep was removed due to the presence of a residual radical signal not completely removed by the pre-saturation pulse. The canonical field positions identified from the field sweep are indicated by arrows.

General chemical synthesis details

Unless stated otherwise, all reagents were obtained from commercial sources and used as received without further purification. Diethyl ether, chloroform and toluene were dried by passing through activated alumina columns using a positive pressure of dry N_2. Diisopropylamine (DIPA) was dried by distillation from CaH_2. All uses of petroleum ether refer to the 40–60 °C fraction. Analytical gel permeation chromatography (GPC) was performed on a JAIGEL H-P precolumn, a JAIGEL 3H-A (8 mm × 500 mm) and a JAIGEL 4H-A column (8 mm × 500 mm) in series with toluene/pyridine 100/1 as eluent. Preparative gel permeation chromatography (GPC) was performed using a line of PLGel 600 mm 10 μm 500 Å, 300 mm 10 μm 500 Å, and 300 mm 10 μm 1000 Å columns (all with 25 mm ID) (Polymer Laboratories Ltd) at a flow rate of 8.5 mL min^{-1}. Preparative recycling GPC was performed on a JAIGEL H-P precolumn, a JAIGEL 3H (20 mm × 600 mm) and a JAIGEL 4H column (20 mm × 600 mm) in series with toluene/pyridine 100/1 as eluent. Flash column chromatography was performed on Merck silica gel 60 (40–63 μm). Alumina columns were performed using aluminum oxide, activated, basic, Brockmann I, standard grade, ~150 mesh, 58 Å from Sigma Aldrich. For TLC, Merck silica gel 60 F_{254} aluminum-backed sheets were used. Size exclusion chromatography (SEC) was carried out using Bio-Beads SX-1, 200–400 mesh (Bio Rad).

Hexakis-(4-[4-phenylpyridine])benzene[13] (**T6**), [5,15-bis(3,5(trihexylsilyl)phenyl)-10,20-dibromoporphyrinato] zinc(II)[14] (**1**) and trihexylsilylacetylene[15] were synthesized according to literature procedures.

NMR spectra were recorded on a Bruker AVII400 or Bruker AVIII400 (400 MHz) spectrometer. The residual solvent peak was used as internal reference (chloroform, ^1H δ = 7.26 ppm, ^{13}C δ = 77.2 ppm). Multiplicity (s = singlet, d = doublet, t = triplet, q = quartet, and m = multiplet) and coupling constant(s) were reported whenever possible. MALDI-TOF-MS spectra were measured using a Waters MALDI Micro MX or at the EPSRC National Mass Spectrometry service (Swansea, Wales, UK) using the Applied Biosystems Voyager DE-STR. UV-vis absorption spectra were recorded at ambient temperature with a Perkin-Elmer Lambda 20 using quartz 1 cm cuvettes. Absorptions appearing as shoulders are annotated "sh".

Schemes S1–S3 describe the synthetic strategies for the preparation of porphyrin oligomers (Scheme S1), preparation of cyclic oligomers (Scheme S2) and preparation of free-base linear oligomers (Scheme S3).

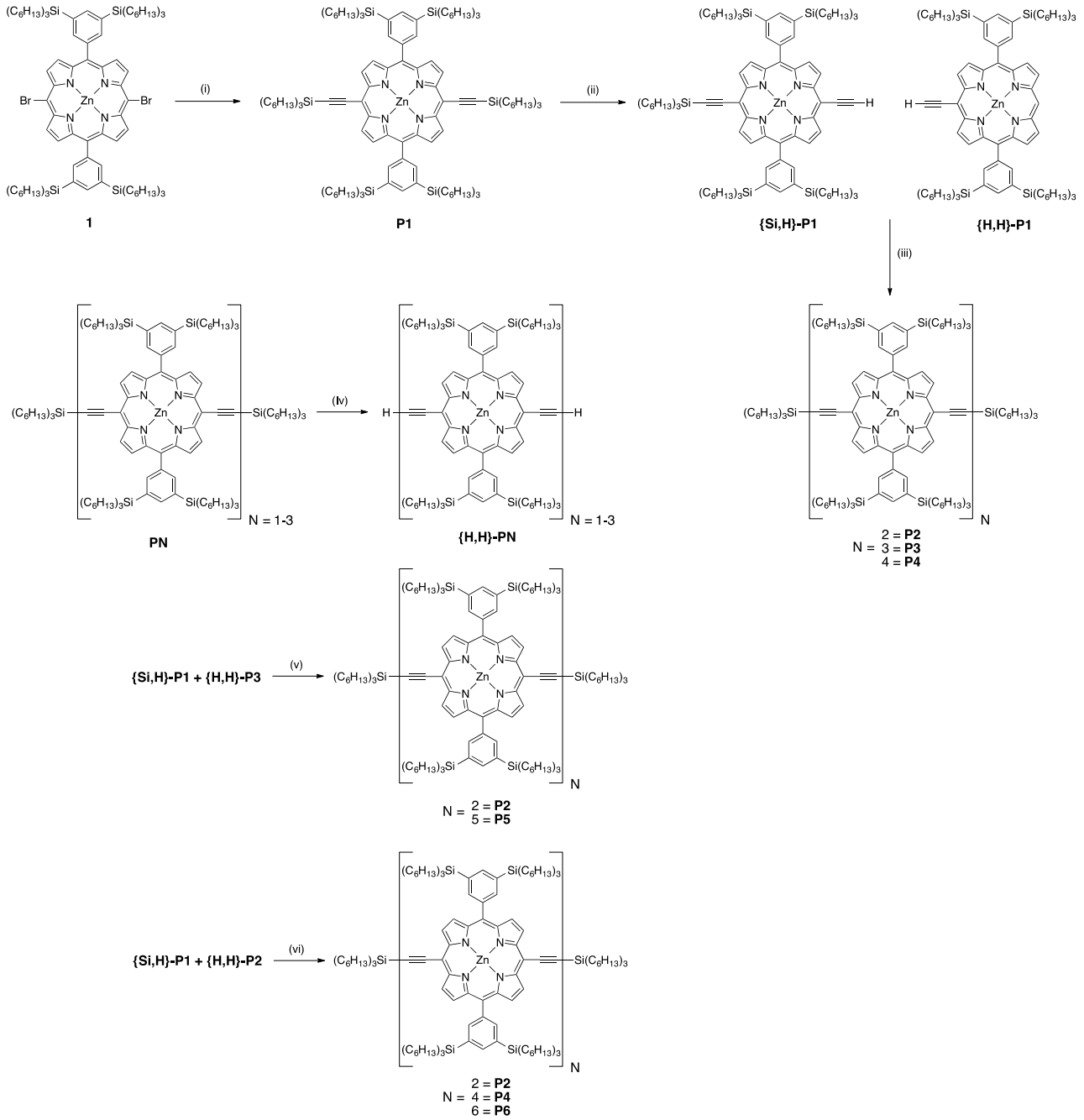

Scheme S1. Preparation of linear porphyrin oligomers **P1**–**P6**.
Reagents and conditions: (i) trihexylsilylacetylene, $Pd_2(dba)_3$, CuI, PPh_3, toluene, DIPA, 50 °C, 2 h, 92%; (ii) TBAF, $CHCl_3$, CH_2Cl_2, pyridine, 20 °C; (iii) $PdCl_2(PPh_3)_2$, CuI, 1,4-benzoquinone, toluene, DIPA, 20 °C, 16 h; (iv) TBAF, $CHCl_3$, pyridine, 20 °C; (v) $PdCl_2(PPh_3)_2$, CuI, 1,4-benzoquinone, toluene, DIPA, 20 °C, 2 h; (vi) $PdCl_2(PPh_3)_2$, CuI, 1,4-benzoquinone, toluene, DIPA, 40 °C, 1.5 h.

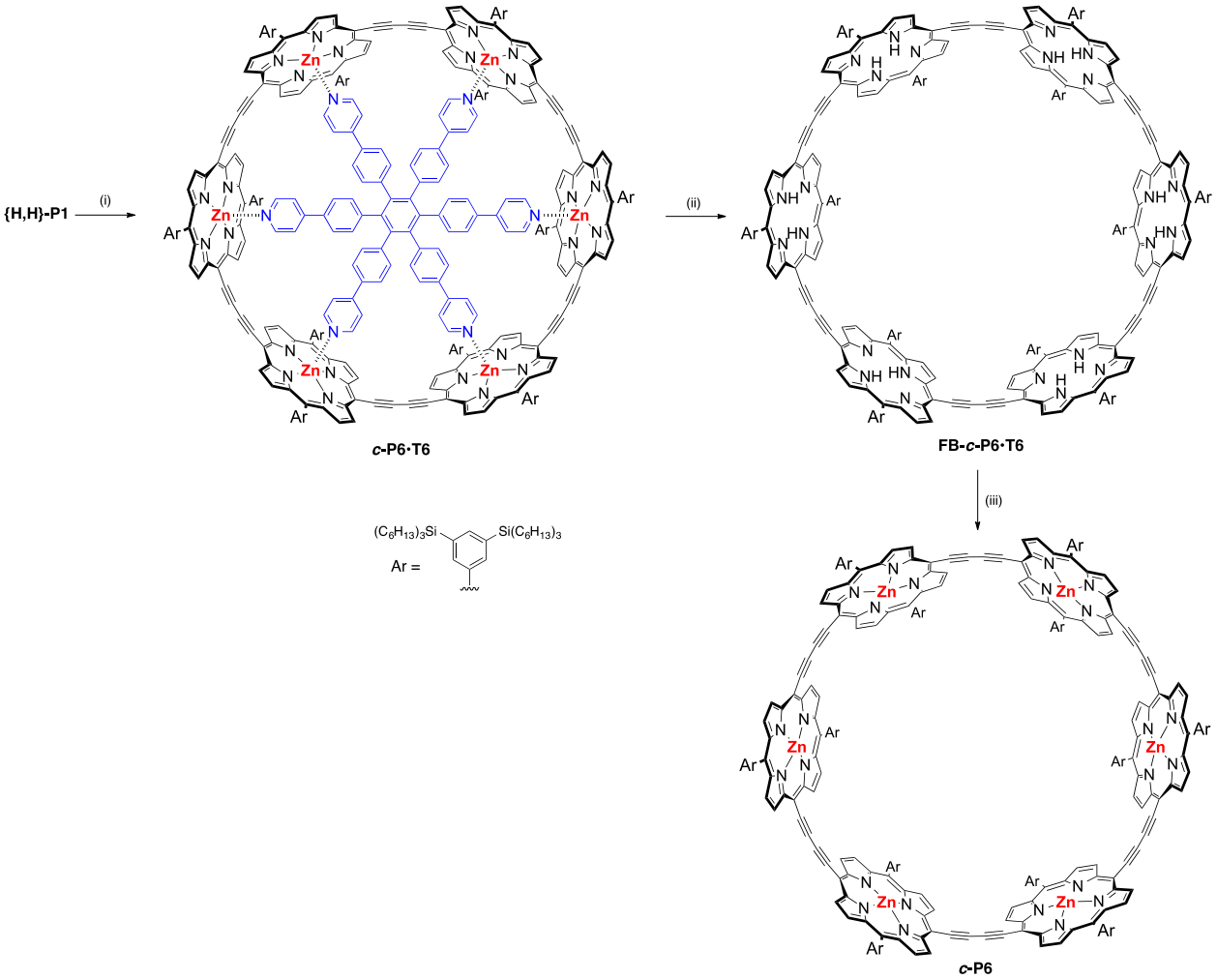

Scheme S2. Preparation of porphyrin nanoring ***c*-P6·T6** and its derivatives.
Reagents and conditions: (i) hexapyridyl template **T6**,[13] $Pd(PPh)_3Cl_2$, CuI, 1,4-benzoquinone, $CHCl_3$, DIPA, 20 °C, 16 h, 36%; (ii) TFA, CH_2Cl_2, 20 °C, 5 min, quant.; (iii) $Zn(OAc)_2 \cdot 2H_2O$, $CHCl_3$, MeOH, 20 °C, 6 h, quant.

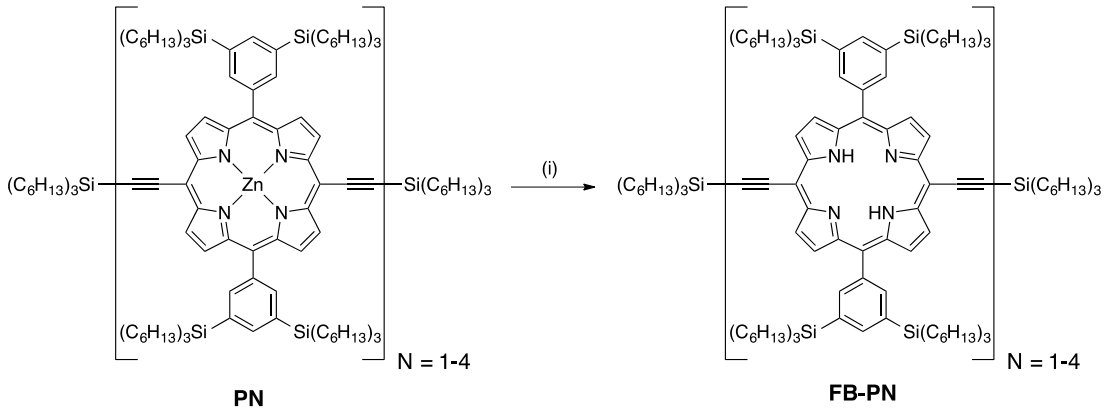

Scheme S3. Demetallation of linear porphyrin oligomers.
Reagents and conditions: (i) TFA, CH_2Cl_2, 20 °C.

Zinc 5,15-bis(3,5-bis-trihexylsilanyl-phenyl)-10,20-bis-trihexylsilanylethynyl-porphyrin (P1)

[5,15-Bis(3,5(trihexylsilyl)phenyl)-10,20-dibromoporphyrinato]zinc(II)[14] **1** (1.42 g, 0.78 mmol), tris-(dibenzylideneacetone)-di-palladium(0) (72 mg, 78 µmol), copper(I) iodide (30 mg, 156 µmol) and triphenylphosphine (41 mg, 156 µmol) were dissolved in a mixture of toluene (35 mL) and DIPA (35 mL) and the solution was degassed by several freeze-pump-thaw cycles. Trihexylsilylacetylene[15] (0.91 mL, 2.3 mmol) was added by syringe and the mixture was stirred at 50 °C for 2 h. TLC indicated full conversion. The reaction mixture was filtered over a plug of silica eluting with PE/DCM 4:1. Purification by column chromatography on silica gel (gradient of petroleum ether/CH_2Cl_2 100:0 to 100:6) yielded **P1** (1.64 g, 92%) as a green oil. ^{1}H NMR (400 MHz, $CDCl_3$): δ = 9.74 (d, ^3J = 4.7 Hz, 4H; ArH_β), 8.90 (d, ^3J = 4.7 Hz, 4H; ArH_β), 8.25 (m, 4H; ArH_{ortho}), 8.00 (m, 2H; ArH_{para}), 1.82–1.69 (m, 12H; CH_2), 1.59–1.44 (m, 36H; CH_2), 1.44–1.25 (m, 96H; CH_2), 1.06–0.98 (m, 12H; CH_2), 0.98–0.91 (m, 24H; CH_2), 0.91–0.83 (m, 54H; CH_3); MS (MALDI-TOF) m/z: calcd. M^+ for $C_{144}H_{248}N_4Si_6Zn$: 2269.49; found: 2270.6; UV-vis (CH_2Cl_2) λ_{max} [nm] (ε [M^{-1} cm^{-1}]): 625 (44,000), 578 (18,000), 446 (323,000), 437 (490,000).

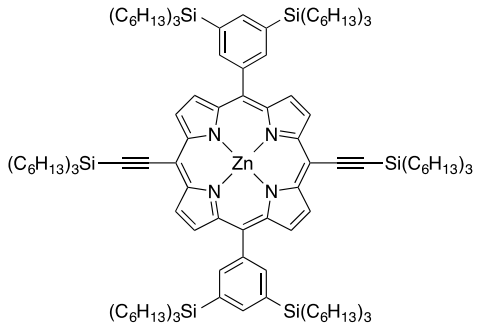

Zinc 5,15-bis(3,5-bis-trihexylsilanyl-phenyl)-10-ethynyl-20-trihexylsilanylethynyl-porphyrin ({Si,H}-P1) and Zinc 5,15-bis(3,5-bis-trihexylsilanyl-phenyl)-10,20-bis-ethynyl-porphyrin ({H,H}-P1)

P1 (863 mg, 0.380 mmol) was dissolved in CH_2Cl_2 (60 mL), chloroform (30 mL) and pyridine (7 mL). The solution was deoxygenated by bubbling argon through the solution. The solution was cooled in a water-ice bath and TBAF (570 µL, 1.0 M in THF, 0.57 mmol) was added. The mixture was stirred and frequently monitored by TLC (petroleum ether/CH_2Cl_2 20/1). As soon as the preferred ratio of deprotection was reached the reaction was quenched with acetic acid (4.2 µL) and the mixture was filtered through a short column of silica gel (CH_2Cl_2 with 1% pyridine). Separation by column chromatography on silica gel (gradient of petroleum ether to petroleum ether/CH_2Cl_2 10/1, always with 1% pyridine) yielded starting material **P1** (133 mg, 15.4%), **{Si,H}-P1** (370 mg, 48%), and **{H,H}-P1** (232 mg, 35%), each as green waxy solids.

{Si,H}-P1: ^{1}H NMR (400 MHz, $CDCl_3$): δ = 9.73 (m, 4H; ArH_β), 8.93 (m, 4H; ArH_β), 8.26 (m, 4H; ArH_{ortho}), 8.00 (m, 2H; ArH_{para}), 4.18 (s, 1H; CH), 1.76 (m, 6H; CH_2), 1.59–1.43 (m, 30H; CH_2),1.43–1.22 (m, 84H; CH_2), 1.06–0.98 (m, 6H; CH_2), 0.98–0.90 (m, 24H; CH_2), 0.90–0.84 (m, 45H; CH_3); MS (MALDI-TOF) *m/z:* calcd. M^+ for $C_{126}H_{210}N_4Si_5Zn$: 1986.9; found: 1989.0.

{H,H}-P1: ^{1}H NMR (400 MHz, $CDCl_3$): δ = 9.75 (d, ^3J = 4.8 Hz, 4H), 8.96 (d, ^3J = 4.8 Hz, 4H), 8.27 (s, 4H), 8.01 (s, 2H), 4.19 (s, 2H), 0.86–1.50 (m, 156H); ^{13}C NMR (100 MHz, $CDCl_3$): δ = 152.3, 150.7, 140.6, 140.2, 139.2, 135.1, 131.2, 123.9, 100.1, 85.9, 83.9, 33.6, 31.7, 24.1, 22.7, 14.2, 12.7, 0.30; MS (MALDI-TOF) *m/z*: calcd. M^+ for $C_{108}H_{172}N_4Si_4Zn$: 1704.31; found: 1703.02; UV-vis (CH_2Cl_2) λ_{max} [nm] ($\log_{10}\varepsilon$): 430 (5.53), 438 (5.47), 568 (4.23), 612 (4.26).

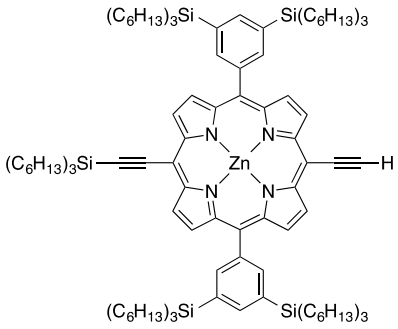

{Si,H}-P1

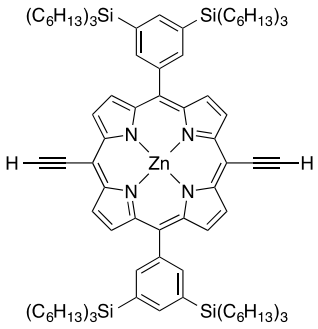

{H,H}-P1

Zinc 5,15-bis(3,5-bis-trihexylsilanyl-phenyl)-10,20-bis-trihexylsilanylethynyl-porphyrin dimer (P2)

{Si,H}-P1 (20 mg, 9.9 µmol) was dissolved in dry toluene (1 mL). $PdCl_2(PPh_3)_2$ (0.4 mg, 0.5 µmol), copper(I) iodide (1.0 mg, 5 µmol), and 1,4-benzoquinone (2.2 mg, 20 µmol) were dissolved in a mixture of dry toluene (1 mL) and dry DIPA (0.5 mL) and added. The reaction was monitored by TLC. After 45 min, all **{Si,H}-P1** had reacted. The volume was reduced and the mixture was filtered through a short column of silica gel (CH_2Cl_2 and 1% pyridine). The mixture was passed through a SEC column (toluene). Recrystallization of the dimer by layer addition (CH_2Cl_2/methanol) yielded **P2** (17 mg, 87%). ^{1}H NMR (400 MHz, $CDCl_3$): δ = 9.94 (d, ^3J = 4.7 Hz, 4H; ArH_β), 9.72 (d, ^3J = 4.7 Hz, 4H; ArH_β), 9.00 (d, ^3J = 4.7 Hz, 4H; ArH_β), 8.92 (d, ^3J = 4.7 Hz, 4H; ArH_β), 8.30 (m, 8H; ArH_{ortho}), 8.02 (m, 4H; ArH_{para}), 1.83–1.70 (m, 12H; CH_2), 1.57–1.46 (m, 60H; CH_2), 1.44–1.23 (m, 168H; CH_2), 1.08–1.00 (m, 12H; CH_2), 1.0–0.92 (m, 48H; CH_2), 0.92–0.85 (m, 90H; CH_3); MS (MALDI-TOF) *m/z*: calcd. M^+ for $C_{252}H_{418}N_8Si_{10}Zn_2$: 3971.78; found: 3974.4; UV-vis (CH_2Cl_2) λ_{max} [nm] (ε

[M^{-1} cm^{-1}]): 708 (114,000), 652 (64,000), 576 (23,000), 488 (219,000), 454 (382,000).

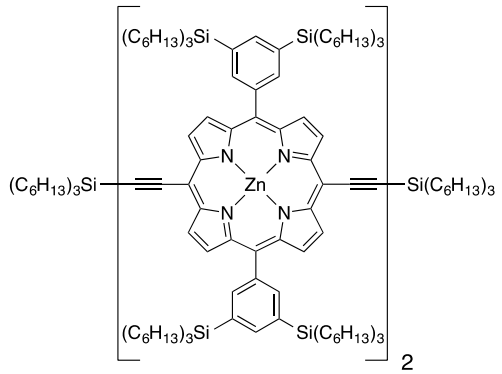

P2

5,15-bis(3,5-bis-trihexylsilanyl-phenyl)-10,20-bis-trihexylsilanylethynyl-porphyrin dimer (P2);

Zinc 5,15-bis(3,5-bis-trihexylsilanyl-phenyl)-10,20-bis-trihexylsilanylethynyl-porphyrin trimer (P3);

Zinc 5,15-bis(3,5-bis-trihexylsilanyl-phenyl)-10,20-bis-trihexylsilanylethynyl-porphyrin tetramer (P4)

A mixture of **{Si,H}-P1** (300 mg, 150 µmol) and **{H,H}-P1** (64 mg, 38 µmol) was dissolved in toluene (25 mL). $PdCl_2(PPh_3)_2$ (15.8 mg, 22 µmol), copper(I) iodide (43 mg, 220 µmol), and 1,4-benzoquinone (33 mg, 300 µmol) were dissolved in a mixture of toluene (10 mL) and DIPA (2.5 mL) and added. The mixture was stirred overnight at room temperature. The reaction mixture was concentrated and filtered through a short column of silica gel (CH_2Cl_2). The mixture was passed through a SEC column (toluene) and then the oligomers were separated by preparative GPC (toluene/pyridine 10/1). Recrystallization of the GPC fractions by layer addition (CH_2Cl_2/methanol) yielded **P2** (66 mg, 22%), **P3** (37 mg, 9%), and **P4** (8.5 mg, 2%), (yields relative to **{Si,H}-P1**).

P3:

^{1}H NMR (400 MHz, $CDCl_3$): δ = 9.95 (d, ^3J = 4.6 Hz, 4H; ArH_β), 9.94 (d, ^{3}J = 4.6 Hz, 4H; ArH_β), 9.72 (d, ^3J = 4.6 Hz, 4H; ArH_β), 9.02 (d, ^3J = 4.6 Hz, 4H; ArH_β), 9.01 (d, ^3J = 4.6 Hz, 4H; ArH_β), 8.91 (d, ^3J = 4.6 Hz, 4H; ArH_β), 8.35 (m, 4H; ArH_{ortho}), 8.31 (m, 8H; ArH_{ortho}), 8.05 (m, 2H; ArH_{para}), 8.03 (m, 4H; ArH_{para}), 1.83–1.70 (m, 12H; CH_2), 1.60–1.46 (m, 84H; CH_2), 1.44–1.23 (m, 240H; CH_2), 1.08–1.00 (m, 12H; CH_2), 1.0–0.92 (m, 72H; CH_2), 0.92–0.85 (m, 126H; CH_3); MS (MALDI-TOF) *m/z*: calcd. M^+ for $C_{360}H_{588}N_{12}Si_{14}Zn_3$: 5674.08; found: 5674.1; UV-vis (CH_2Cl_2) λ_{max} [nm] (ε [M^{-1} cm^{-1}]): 738 (173,000), 501 (31,000), 492 (255,000), 453 (436,000).

P4:

^{1}H NMR (400 MHz, $CDCl_3$): δ = 9.98 (m, 12H; ArH_β), 9.74 (d, ^3J = 4.6 Hz, 4H; ArH_β), 9.06 (m, 8H; ArH_β), 9.03 (d, ^3J = 4.6 Hz, 4H; ArH_β), 8.94 (d, ^3J = 4.6 Hz, 4H; ArH_β), 8.37 (m, 8H; ArH_{ortho}), 8.32 (m, 8H; ArH_{ortho}), 8.06 (m, 4H; ArH_{para}), 8.04 (m, 4H; ArH_{para}), 1.83–1.70 (m, 12H; CH_2), 1.60–1.46 (m, 108H; CH_2), 1.44–1.23 (m, 312H; CH_2), 1.07–0.94 (m, 108H; CH_2), 0.94–0.85 (m, 162H; CH_3); MS (MALDI-TOF) *m/z*: calcd. M^+ for $C_{468}H_{758}N_{16}Si_{18}Zn_4$: 7376.37; found: 7379; UV-vis (CH_2Cl_2) λ_{max} [nm] (ε [M^{-1} cm^{-1}]): 761 (241,000), 747 (240,000), 581 (44,000), 491 (404,000), 452 (520,000).

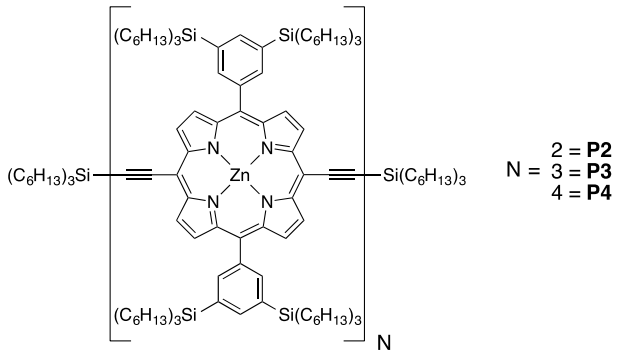

Zinc 5,15-bis(3,5-bis-trihexylsilanyl-phenyl)-10,20-bis-ethynyl-porphyrin dimer ({H,H}-P2)

TBAF (100 µL, 1.0 M in THF, 100 µmol) was added to a solution of **P2** (45 mg, 11 µmol) in CH_2Cl_2 (20 mL) and the mixture was stirred for 1 h at room temperature. The reaction was monitored by TLC. After the deprotection was complete, acetic acid (1 mL) was added and the mixture was passed through a short column of silica gel (CH_2Cl_2). Removing the solvent yielded **{H,H}-P2** (39 mg, 99%) as a green waxy solid. ^{1}H NMR (400 MHz, $CDCl_3$): δ = 9.97 (d, ^3J = 4.7 Hz, 4H; ArH_β), 9.75 (d, ^3J = 4.7 Hz, 4H; ArH_β), 9.04 (d, ^3J = 4.7 Hz, 4H; ArH_β), 8.96 (d, ^3J = 4.7 Hz, 4H; ArH_β), 8.13 (m, 8H; ArH_{ortho}), 8.02 (m, 4H; ArH_{para}), 4.22 (s, 2H; CH), 1.57–1.46 (m, 48H; CH_2), 1.44–1.23 (m, 144H; CH_2), 1.0–0.92 (m, 48H; CH_2), 0.92–0.85 (m, 72H; CH_3); MS (MALDI-TOF) *m/z*: calcd. M^+ for $C_{216}H_{342}N_8Si_8Zn_2$: 3406.61; found: 3406.6.

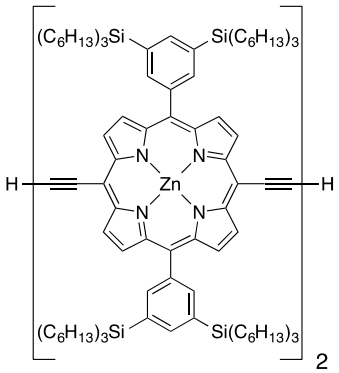

{H,H}-P2

Zinc 5,15-bis(3,5-bis-trihexylsilanyl-phenyl)-10,20-bis-ethynyl-porphyrin trimer ({H,H}-P3)

TBAF (50 µL, 1.0 M in THF, 50 µmol) was added to a solution of **P3** (21 mg, 3.7 µmol) in CH_2Cl_2 (21 mL) and the mixture was stirred for 1 h at room temperature. The reaction was monitored by TLC. After the deprotection was complete acetic acid (1 mL) was added and the mixture was passed through a short column of silica gel (CH_2Cl_2). Removing the solvent yielded **{H,H}-P3** (17 mg, 89%) as an olive green solid. ^{1}H NMR (400 MHz, $CDCl_3$): δ = 9.99 (d, ^3J = 4.7 Hz, 4H; ArH_β), 9.97 (d, ^3J = 4.7 Hz, 4H; ArH_β), 9.76 (d, ^3J = 4.7 Hz, 4H; ArH_β), 9.06 (d, ^3J = 4.7 Hz, 4H; ArH_β), 9.05 (d, ^3J = 4.7 Hz, 4H; ArH_β), 8.97 (d, ^3J = 4.7 Hz, 4H; ArH_β), 8.36 (m, 4H;

ArH_{ortho}), 8.32 (m, 8H; ArH_{ortho}), 8.05 (m, 2H; ArH_{para}), 8.04 (m, 4H; ArH_{para}), 4.22 (s, 2H; CH), 1.58–1.46 (m, 72H; CH_2), 1.45–1.24 (m, 216H; CH_2), 1.02–0.93 (m, 72H; CH_2), 0.93–0.85 (m, 108H; CH_3); MS (MALDI-TOF) *m/z*: calcd. M^+ for $C_{324}H_{512}N_{12}Si_{12}Zn_3$: 5108.90; found: 5108.4.

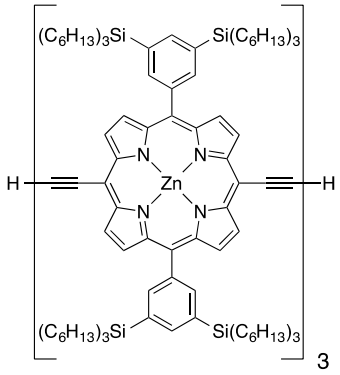

{H,H}-P3

Zinc 5,15-bis(3,5-bis-trihexylsilanyl-phenyl)-10,20-bis-trihexylsilanylethynyl-porphyrin pentamer (P5)

A solution of $PdCl_2(PPh_3)_2$ (10 mg, 14 µmol), copper(I) iodide (28 mg, 147 µmol) and 1,4-benzoquinone (22 mg, 200 µmol) in toluene (10 mL) and DIPA (1.5 mL) was added to a stirred mixture of **{Si,H}-P1** (65 mg, 33 µmol) and **{H,H}-P3** (15 mg, 3 µmol) in toluene (10 mL). The mixture was stirred for 2 h at room temperature, then the solvent was removed and the mixture was filtered over a short column of silica gel (CH_2Cl_2/petroleum ether 1/1). Purification by preparative GPC (toluene/pyridine 10/1) and subsequent recrystallization by layer addition (CH_2Cl_2/methanol) yielded **P2** (37 mg, 28% relative to **{Si,H}-P1**) and **P5** (8 mg, 30% relative to **{H,H}-P3**).

P5:

^{1}H NMR (400 MHz, $CDCl_3$): δ = 9.97 (m, 16H; ArH_β), 9.73 (d, ^3J = 4.6 Hz, 4H; ArH_β), 9.05 (m, 12H; ArH_β), 9.02 (d, ^3J = 4.6 Hz, 4H; ArH_β), 8.92 (d, ^3J = 4.6 Hz, 4H; ArH_β), 8.37 (m, 12H; ArH_{ortho}), 8.31 (m, 8H; ArH_{ortho}), 8.06 (m, 6H; ArH_{para}), 8.03 (m, 4H; ArH_{para}), 1.83–1.70 (m, 12H; CH_2), 1.60–1.46 (m, 132H; CH_2), 1.45–1.24 (m, 384H; CH_2), 1.07–0.94 (m, 132H; CH_2), 0.94–0.85 (m, 198H; CH_3); MS (MALDI-TOF) *m/z*: calcd. M^+ for $C_{576}H_{928}N_{20}Si_{22}Zn_5$: 9078.67; found: 9083; UV-vis (CH_2Cl_2) λ_{max} [nm] (ε [M^{-1} cm^{-1}]): 769 (320,000), 581 (49,000), 491 (499,000), 452 (579,000).

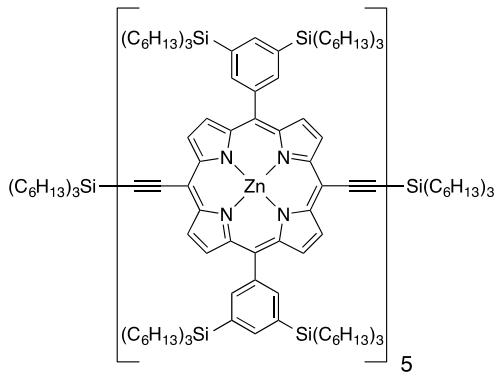

P5

Zinc 5,15-bis(3,5-bis-trihexylsilanyl-phenyl)-10,20-bis-trihexylsilanylethynyl-porphyrin hexamer (P6)

A solution of $PdCl_2(PPh_3)_2$ (8.0 mg, 11 µmol), copper(I) iodide (20 mg, 100 µmol) and 1,4-benzoquinone (15 mg, 140 µmol) in toluene (5 mL) and DIPA (1 mL) was added to a stirred mixture of **{Si,H}-P1** (42 mg, 22 µmol) and **{H,H}-P2** (38 mg, 11 µmol) in toluene (10 mL). The mixture was stirred for 1.5 h at 40 °C, then the solvent was removed and the mixture was filtered over a short column of silica gel (CH_2Cl_2/petroleum ether 1/1). Purification by preparative GPC (toluene/pyridine 10/1) and subsequent recrystallization by layer addition (CH_2Cl_2/methanol) yielded **P2** (13.5 mg, 31% relative to **{Si,H}-P1**), **P4** (4.2 mg, 5% relative to **{H,H}-P2**), and **P6** (2.1 mg, 4% relative to **{H,H}-P2**).

P6:

^{1}H NMR (400 MHz, $CDCl_3$): δ = 9.98 (m, 20H; ArH_β), 9.74 (d, ^3J = 4.6 Hz, 4H; ArH_β), 9.06 (m, 16H; ArH_β), 9.03 (d, ^3J = 4.6 Hz, 4H; ArH_β), 8.93 (d, ^3J = 4.6 Hz, 4H; ArH_β), 8.37 (m, 16H; ArH_{ortho}), 8.31 (m, 8H; ArH_{ortho}), 8.06 (m, 8H; ArH_{para}), 8.03 (m, 4H; ArH_{para}), 1.83–1.70 (m, 12H; CH_2), 1.60–1.46 (m, 156H; CH_2), 1.46–1.24 (m, 456H; CH_2), 1.07–0.94 (m, 156H; CH_2), 0.94–0.85 (m, 234H; CH_3); MS (MALDI-TOF) *m/z*: calcd. M^+ for $C_{684}H_{1098}N_{24}Si_{26}Zn_6$: 10780.97; found: 10783; UV-vis (CH_2Cl_2) λ_{max} [nm] (ε [M^{-1} cm^{-1}]): 776 (404,000), 582 (61,000), 491 (636,000), 453 (698,000).

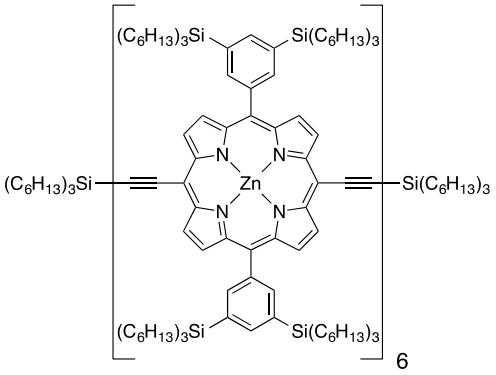

P6

Zinc (3,5-bis-trihexylsilanyl-phenyl)-porphyrin[6] nanoring–template complex (*c*-P6•T6)

{H,H}-P1 (200 mg, 0.120 mmol) and template **T6**[13] (29 mg, 29 µmol) were dissolved in chloroform (133 mL) by sonication for 2 h A solution of $Pd(PPh_3)_2Cl_2$ (27 mg, 39 µmol), copper(I) iodide (37 mg, 0.19 mmol) and 1,4-benzoquinone (89 mg, 0.80 mmol) in chloroform (18 mL) and DIPA (0.25 mL) was added to the porphyrin mixture, at room temperature. The mixture was stirred at room temperature overnight, open to air. The reaction mixture was partially concentrated and passed over a plug of alumina ($CHCl_3$). Purification by SEC (toluene) and preparative recycling GPC (toluene + 1% pyridine) afforded ***c*-P6•T6** (78 mg, 36%) as a brown solid. ^{1}H NMR (400 MHz, $CDCl_3$): δ = 9.54 (d, ^3J = 4.4 Hz, 24H; ArH_β), 8.72 (d, ^3J = 4.4 Hz, 24H; ArH_β), 8.37 (m, 12H; ArH_{ortho}), 8.32 (m, 12H; ArH_{ortho}), 8.06 (m, 12H; ArH_{para}), 5.52 (m, 12H; AA' phenyl), 5.45 (m, 12H; BB' phenyl), 4.99 (m, 12H; AA' pyridine), 2.41 (m, 12H;

XX' pyridine), 1.56–1.41 (m, 144H; C*H*$_2$), 1.41–1.17 (m, 432H; CH_2), 1.00–0.75 (m, 360H; CH_2, CH_3); MS (MALDI-TOF) *m/z*: calcd. M^+ for $C_{720}H_{1068}N_{30}Si_{24}Zn_6$: 11211; found: 11207. UV-vis (CH_2Cl_2) λ_{max} [nm] (ε [M^{-1} cm^{-1}]): 850 (404,000), 808 (496,000), 772 (374,000), 612 (39,000), 482 (570,000).

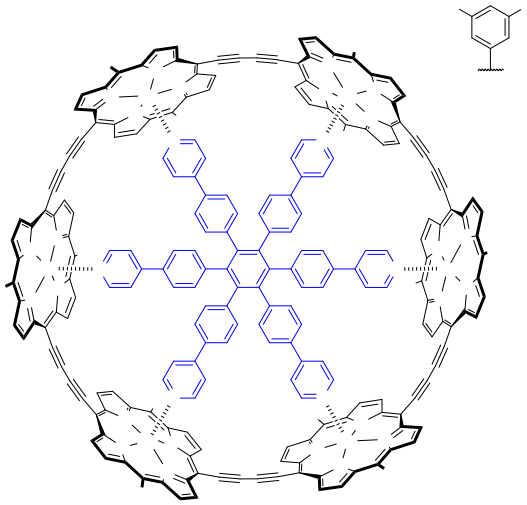

.

Free base (3,5-bis-trihexylsilanyl-phenyl)-porphyrin[6] nanoring (FB-*c*-P6)

***c*-P6·T6** (5.4 mg, 0.48 μmol) was dissolved in CH_2Cl_2 (5 mL) and trifluoroacetic acid (50 μL, 0.65 mmol) was added. The mixture was stirred for 5 min. at room temperature then pyridine (0.5 mL) was added and the mixture was immediately filtered over a short column of silica gel (CH_2Cl_2). Removing the solvent yielded **FB-*c*-P6** (4.8 mg, 100%) as a green solid. ^{1}H NMR (400 MHz, $CDCl_3$): δ = 9.56 (d, ^3J = 4.7 Hz, 24H; ArH_β), 8.71 (d, ^3J = 4.7 Hz, 24H; ArH_β), 8.15 (m, 24H; ArH_{ortho}), 7.96 (m, 12H; ArH_{para}), 1.52–1.36 (m, 144H; CH_2), 1.36–1.14 (m, 432H; CH_2), 1.07–0.94 (m, 144H; CH_2), 0.94–0.85 (m, 216H; CH_3), –1.29 (s, 12H; NH); MS (MALDI-TOF) *m/z*: calcd. M^+ for $C_{648}H_{1032}N_{24}Si_{24}$: 9834; found: 9836; UV-vis (CH_2Cl_2) λ_{max} [nm] (ε [M^{-1} cm^{-1}]) = 791 (296,000), 771 (311,000), 659 (199,000), 466 (519,000).

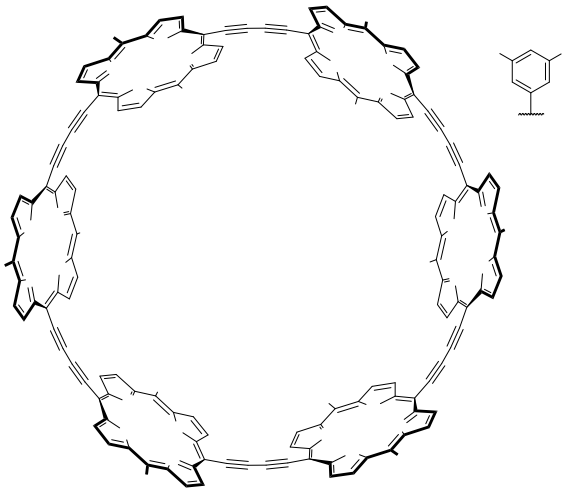

Zinc (3,5-bis-trihexylsilanyl-phenyl)-porphyrin[6] nanoring (*c*-P6)

FB-*c*-P6 (4.8 mg, 0.48 μmol) was dissolved in CH_2Cl_2 (10 mL) and a solution of $Zn(OAc)_2$•$2H_2O$ (50 mg, 228 μmol) in methanol (2 mL) was added. The mixture was stirred over night at room temperature then filtered through a short column of silica gel (CH_2Cl_2). Recrystallization by layer addition (CH_2Cl_2/methanol) yielded ***c*-P6** (4.9 mg, 100%) as a brown solid. ^{1}H NMR (400 MHz, $CDCl_3$): δ = 9.67 (d, ^3J = 4.6 Hz, 24H; ArH_β), 8.81 (d, ^3J = 4.6 Hz, 24H; ArH_β), 8.16 (m, 24H; ArH_{ortho}), 7.91 (m, 12H; ArH_{para}), 1.50–1.37 (m, 144H; CH_2), 1.37–1.12 (m, 432H; CH_2), 0.94–0.84 (m, 144H; CH_2), 0.84–0.72 (m, 216H; CH_3); MS (MALDI-TOF) *m/z*: calcd. M^+ for $C_{648}H_{1020}N_{24}Si_{24}Zn_6$: 10214; found: 10211; UV-vis (CH_2Cl_2) λ_{max} [nm] (ε [M^{-1} cm^{-1}]): 772 (285,000), 748 (307,000), 593 (42,000), 473 (516,000).

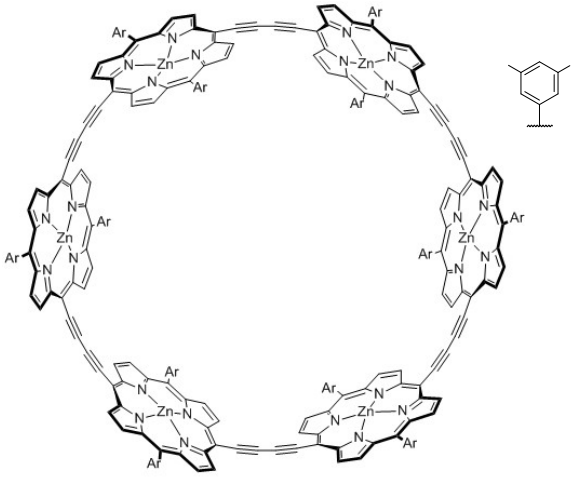

***c*-P6**

General Procedure 1: TFA demetallation of zinc porphyrin oligomers

TFA (100 eq. per Zn, ~0.5 vol% *vs.* $CHCl_3$) was added to a solution of porphyrin substrate (1 eq.) in $CHCl_3$ (~0.1–0.5 mM). The reaction mixture was monitored by UV-vis spectroscopy, diluting aliquots in CH_2Cl_2/1% pyridine. Upon completion, the reaction mixture was quenched by addition of pyridine and was immediately passed through a SiO_2 plug (CH_2Cl_2 + 1% pyridine). Purification by flash chromatography on SiO_2 (petroleum ether) afforded the free-base oligomer.

Free-base 5,15-bis(3,5-bis-trihexylsilanyl-phenyl)-10,20-bis-trihexylsilanylethynyl-porphyrin FB-P1

P1 (10 mg, 4.4 μmol) was subject to general procedure 1 to afford **FB-P1**. ^{1}H NMR (400 MHz, $CDCl_3$): δ = 9.59 (d, ^3J = 4.7 Hz, 4H; ArH_β), 8.76 (d, ^3J = 4.6 Hz, 4H; ArH_β), 8.22 (s, 4H; ArH_{ortho}), 7.99 (s, 2H; ArH_{para}), 1.78–1.67 (m, 11H), 1.57–1.21 (m, 132H), 1.04–0.80 (m, 92H), –2.11 (s, 2H; NH); MS (MALDI-TOF) *m/z*: calcd. M^+ for $C_{144}H_{250}N_4Si_6$: 2206.12; found 2206.64; UV-vis (CH_2Cl_2) λ_{max} [nm]: 433m 442, 583, 677.

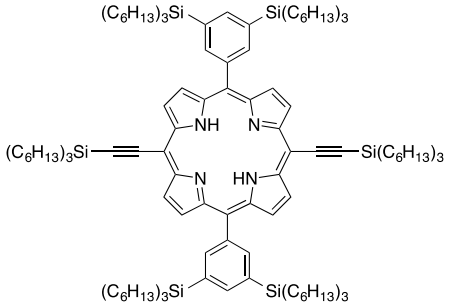

FB-P1

Free-base 5,15-bis(3,5-bis-trihexylsilanyl-phenyl)-10,20-bis-trihexylsilanylethynyl-porphyrin dimer FB-P2

P2 (8.0 mg, 2.0 μmol) was subject to general procedure 1 to afford **FB-P2**. ^{1}H NMR (400 MHz, $CDCl_3$): δ = 9.82 (d, ^3J = 4.6 Hz, 4H; ArH_β), 9.61 (d, ^3J = 4.7 Hz, 4H; ArH_β), 8.88 (d, ^3J = 4.7 Hz; 4H, ArH_β), 8.80 (d, ^3J = 4.7 Hz, 4H; ArH_β), 8.28 (s, 8H; ArH_{ortho}), 8.02 (s, 4H; ArH_{para}), 1.81–1.69 (m, 12H), 1.58–1.23 (m, 229H), 1.06–0.82 (m, 149H), –1.83 (s, 4H; NH). MS (MALDI-TOF) *m/z*: calcd. M^+ for $C_{252}H_{422}N_8Si_{10}$: 3845.05; found: 3844.56; UV-vis (CH_2Cl_2) λ_{max} [nm]: 418 (sh) 442, 474, 600, 621, 690 (sh), 728.

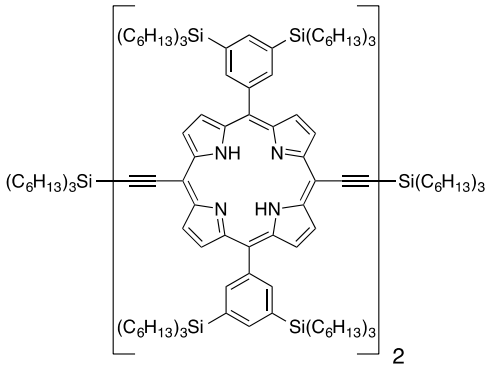

FB-P2

Free-base 5,15-bis(3,5-bis-trihexylsilanyl-phenyl)-10,20-bis-trihexylsilanylethynyl-porphyrin trimer FB-P3

P3 (3.0 mg, 0.53 μmol) was subject to general procedure 1 to afford **FB-P3**. ^{1}H NMR (400 MHz, $CDCl_3$): δ = 9.88–9.79 (m, 8H; ArH_β), 9.61 (d, ^3J = 4.4 Hz, 4H; ArH_β), 8.95–8.85 (m, 8H; ArH_β), 8.80 (d, ^3J = 4.4 Hz, 4H; ArH_β), 8.33 (s, 4H; ArH_{ortho}), 8.28 (s, 8H; ArH_{ortho}), 8.04 (s, 2H; ArH_{para}), 8.02 (s, 4H; ArH_{para}), 1.82–0.97 (m, 546H), –1.56 (s, 2H; NH), –1.82 (s, 4H; NH). MS (MALDI-TOF) *m/z*: calcd. M^+ for $C_{360}H_{594}N_{12}Si_{14}$: 5483.99; found: 5482.42; UV-vis (CH_2Cl_2) λ_{max} [nm]: 428 (sh), 450, 486 (sh), 641, 752, 781 (sh).

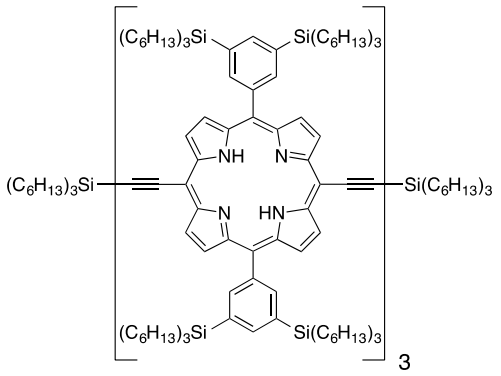

FB-P3

Free-base 5,15-bis(3,5-bis-trihexylsilanyl-phenyl)-10,20-bis-trihexylsilanylethynyl-porphyrin tetramer FB-P4

P4 (3.0 mg, 0.54 μmol) was subject to general procedure 1 to afford **FB-P4**. ^{1}H NMR (400 MHz, $CDCl_3$): δ = 9.85 (m, 12H; ArH_β), 9.62 (d, ^3J = 4.6 Hz, 4H; ArH_β), 8.99–8.87 (m, 12H; ArH_β), 8.81 (d, ^3J = 4.2 Hz, 4H; ArH_β), 8.35 (s, 8H; ArH_{ortho}), 8.30 (s, 8H; ArH_{ortho}), 8.05 (s, 4H; ArH_{para}), 8.02 (s, 4H; ArH_{para}), 1.82–0.76 (m, 702H; CH_3/CH_2), –1.53 (s, 4H; NH), –1.80 (s, 4H; NH). MS (MALDI-TOF) *m/z*: calcd. M^+ for $C_{468}H_{766}N_{16}Si_{18}$: 7122.92; found 7124.11; UV-vis (CH_2Cl_2) λ_{max} [nm]: 450, 477 (sh), 642, 770.

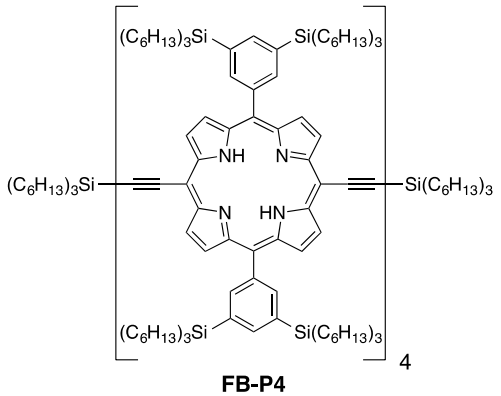

FB-P4

References

1. Stoll, S.; Schweiger, A. *J. Magn. Reson.* **2006**, *178*, 42-55.
2. Siegel, S.; Judeikis, H. S. *J. Phys. Chem.* **1966**, *70*, 2205-2211.
3. Thurnauer, M. C.; Norris, J. R. *Biochem. Biophys. Res. Commun.* **1976**, *73*, 501-506.
4. Neese, F. *ORCA - an ab initio, Density Functional and Semiempirical program package*, 2.9/3.0; 2011.
5. Neese, F. *Wiley Interdiscp. Rev.: Comput. Mol. Sci.* **2012**, *2*, 73-78.
6. Sinnecker, S.; Neese, F. *J. Phys. Chem. A* **2006**, *110*, 12267-12275.
7. Barone, V., In *Recent Advances in Density Functional Methods, Part I*, Chong, D. P., Ed. World Scientific Publ. Co.: Singapore, 1996.
8. Barone, V. *J. Chem. Phys.* **1994**, *101*, 6834-6838.
9. Barone, V. *J. Chem. Phys.* **1994**, *101*, 10666-10676.
10. Ernzerhof, M., Hybrid Methods: Combining Density Functional and Wavefunction Theory. In *Density Functionals: Theory and Applications*, Joubert, D., Ed. Springer: 1998; pp 60-90.
11. Polo, V.; Kraka, E.; Cremer, D. *Mol. Phys.* **2002**, *100*, 1771-1790.
12. Pipek, J.; Mezey, P. *J. Chem. Phys.* **1989**, *90*, 4916-4926.
13. Hoffmann, M.; Kärnbratt, J.; Chang, M.-H.; Herz, L. M.; Albinsson, B.; Anderson, H. L. *Angew. Chem. Int. Ed.* **2008**, *47*, 4993-6.
14. Grozema, F. C.; Houarner-Rassin, C.; Prins, P.; Siebbeles, L. D. A.; Anderson, H. L. *J. Am. Chem. Soc.* **2007**, *129*, 13370-13371.
15. Lehnherr, D.; Gao, J.; Hegmann, F. A.; Tykwinski, R. R. *Org. Lett.* **2008**, *10*, 4779-4782.